**Electronic Supporting Information**

# Surface Carbon Hydrogenation on Pre-covered Fe(110) with Spectators-Coverage-Dependent Chain Initiation and Propagation

Teng Li,[a,b,c] Xiaodong Wen[a,c] Yong-Wang Li,[a,c] and Haijun Jiao[a,d]*

*(a) State Key Laboratory of Coal Conversion, Institute of Coal Chemistry, Chinese Academy of Sciences, Taiyuan, 030001, China; (b) University of Chinese Academy of Sciences, No. 19A Yuquan Road, Beijing, 100049, PR China; (c) National Energy Center for Coal to Liquids, Synfuels China Co., Ltd, Huairou District, Beijing, 101400, China; (d) Leibniz-Institut für Katalyse e.V. an der Universität Rostock, Albert-Einstein Strasse 29a, 18059 Rostock, Germany. haijun.jiao@catalysis.de*

**Content**

Table S1 Reactions summary of ethane and propane formation

| | Reaction | $E_a$/eV | $E_a+E_{zpe}$ /eV | $(E_a+E_{ZPE})$ $-E_a$/eV | $E_r$/eV | $E_r+E_{zpe}$ /eV | $(E_r+E_{ZPE})$ $-E_r$/eV | r(C-H or C-C)/Å | r(Fe-H or Fe-C)/Å | (v/i)/$cm^{-1}$ | k(550 K)/$s^{-1}$ |
|---|---|---|---|---|---|---|---|---|---|---|---|
| 1 | CH+CH+12H+2C→CHCH+12H+2C | 0.49 | 0.48 | −0.01 | −0.36 | −0.32 | 0.04 | 1.848 | 1.864,1.875,2.118; 1.910,1.912,2.001 | 536 | $3.318\times10^{8}$ |
| 2 | CH+CH+12H+2C→$CH_2$+CH+12H+2C | 0.52 | 0.48 | −0.04 | 0.44 | 0.48 | 0.04 | 1.452 | 1.580 | 737 | $1.731\times10^{8}$ |
| 3 | $CH_2$CH+12H+2C→$CH_2CH_2$+11H+2C | 0.52 | 0.47 | −0.05 | −0.17 | −0.07 | 0.10 | 1.568 | 1.562 | 993 | $2.109\times10^{8}$ |
| 4 | $CH_2CH_2$+12H+2C →$CH_2CH_3$+11H+2C | 0.51 | 0.43 | −0.08 | 0.15 | 0.19 | 0.04 | 1.548 | 1.630, 2.134 | 787 | $2.588\times10^{8}$ |
| 5 | $CH_2$CH+12H+2C→$CH_3$CH+11H+2C | 0.48 | 0.43 | −0.05 | 0.03 | 0.09 | 0.06 | 1.520 | 1.624; 2.145 | 852 | $4.031\times10^{8}$ |
| 6 | $CHCH_3$+12H+2C →$CH_2CH_3$+11H+2C | 0.60 | 0.56 | −0.04 | 0.13 | 0.24 | 0.11 | 1.531 | 1.581; 2.038, 2.010, 2.319 | 940 | $3.050\times10^{7}$ |
| 7 | $CH_2CH_3$+12H+2C →$CH_3CH_3$+11H+2C | 0.72 | 0.65 | −0.07 | −0.58 | −0.52 | 0.06 | 1.475 | 1.642; 2.314 | 1066 | $3.182\times10^{6}$ |
| 8 | $CH_3$CH+CH+11H+2C→$CH_3$C+CH+12H+2C | 0.03 | −0.06 | −0.09 | −0.58 | −0.63 | 0.05 | 1.483 | 1.538 | 652 | $5.604\times10^{12}$ |
| 9 | $CH_3$C+CH+12H+2C→$CH_3$C+$CH_2$+11H+2C | 0.59 | 0.56 | −0.03 | 0.37 | 0.43 | 0.06 | 1.494 | 1.549 | 772 | $4.093\times10^{7}$ |
| 10 | $CH_3$C+CH+12H+2C→$CH_3$CCH+11H+2C | 0.60 | 0.60 | 0.00 | −0.25 | −0.21 | 0.04 | 1.880 | 1.846, 1.866 | 453 | $3.219\times10^{7}$ |
| 11 | $CH_3$CCH+12H+2C→$CH_3$CHCH+11H+2C | 0.49 | 0.44 | −0.05 | 0.31 | 0.41 | 0.10 | 1.560 | 1.612 | 858 | $3.519\times10^{8}$ |
| 12 | $CH_3$CCH+12H+2C→$CH_3CCH_2$+11H+2C | 0.82 | 0.77 | −0.05 | 0.33 | 0.43 | 0.10 | 1.533 | 1.706 | 776 | $3.633\times10^{5}$ |
| 13 | $CH_3$CH+CH+12H+2C→$CH_3$CHCH+12H+2C | 0.73 | 0.76 | 0.03 | −0.44 | −0.34 | 0.10 | 1.931 | 1.930 | 424 | $2.145\times10^{6}$ |
| 14 | $CH_3$CHCH+12H+2C→$CH_3CH_2$CH+11H+2C | 0.60 | 0.55 | −0.05 | 0.08 | 0.14 | 0.06 | 1.511 | 1.661 | 790 | $3.413\times10^{7}$ |
| 15 | $CH_3$CHCH+12H+2C→$CH_3CHCH_2$+11H+2C | 0.56 | 0.51 | −0.05 | 0.04 | 0.14 | 0.10 | 1.553 | 1.568 | 996 | $8.557\times10^{7}$ |
| 16 | $CH_3CH_2$CH+12H+2C→$CH_3CH_2CH_2$+11H[a]+2C | 0.64 | 0.58 | −0.06 | 0.25 | 0.34 | 0.09 | 1.523 | 1.575 | 930 | $1.650\times10^{7}$ |
| 17 | $CH_3CHCH_2$+12H+2C→$CH_3CH_2CH_2$+11H[b]+2C | 0.61 | 0.55 | −0.06 | 0.28 | 0.33 | 0.05 | 1.505 | 1.641;2.187 | 890 | $3.018\times10^{7}$ |
| 18 | $CH_3CHCH_2$+12H+2C→$CH_3CHCH_3$+11H+2C | 1.38 | 1.31 | −0.07 | 0.25 | 0.32 | 0.07 | 1.479 | 1.569 | 1063 | 2.625 |
| 19 | $CH_3CH_2CH_2$+12H+2C→$CH_3CH_2CH_3$+11H+2C | 0.67 | 0.62 | −0.05 | −0.68 | −0.62 | 0.06 | 1.517 | 1.658; 2.335 | 1075 | $8.128\times10^{6}$ |

Table S2 Temperature effects on the reaction energies of ethylene and ethane formation

| Reaction 3: $CH_2CH+12H+2C \rightarrow CH_2CH_2+11H+2C$ | | | | Reaction 7: $CH_3CH_2+12H+2C \rightarrow CH_3CH_3+11H+2C$ | | | |
|---|---|---|---|---|---|---|---|
| $\Delta E_{elec}$/eV | | −0.166 | | $\Delta E_{elec}$/eV | | −0.582 | |
| $\Delta(E_{elec}+E_{ZPE})$ | | −0.068 | | $\Delta(E_{elec}+E_{ZPE})$ | | −0.517 | |
| $\Delta H \sim T$ | | | | $\Delta H \sim T$ | | | |
| $T$/K | $\Delta H$/eV | $\Delta H$-$\Delta E_{elec}$/eV | $\Delta H$-$\Delta(E_{elec}$-$E_{ZPE})$/eV | $T$/K | $\Delta H$/eV | $\Delta H$-$\Delta E_{elec}$/eV | $\Delta H$-$\Delta(E_{elec}$-$E_{ZPE})$/eV |
| 250 | −0.054 | 0.112 | 0.014 | 250 | −0.496 | 0.086 | 0.021 |
| 300 | −0.053 | 0.113 | 0.015 | 300 | −0.496 | 0.086 | 0.021 |
| 350 | −0.052 | 0.114 | 0.016 | 350 | −0.498 | 0.084 | 0.019 |
| 400 | −0.052 | 0.114 | 0.016 | 400 | −0.500 | 0.082 | 0.017 |
| 450 | −0.053 | 0.113 | 0.015 | 450 | −0.504 | 0.078 | 0.013 |
| 500 | −0.054 | 0.112 | 0.014 | 500 | −0.508 | 0.074 | 0.009 |
| 550 | −0.055 | 0.111 | 0.013 | 550 | −0.513 | 0.069 | 0.004 |
| 600 | −0.057 | 0.109 | 0.011 | 600 | −0.518 | 0.064 | −0.001 |

The formation enthalpy ($\Delta H$) of reaction is composed by three parts: the electronic energy ($E_{elec}$), the zero point correction ($E_{ZPE}$), the integration of heat capacity at constant volume from 0 K to real temperature. (Grabow, Lars C. "Computational catalyst screening. "Computational Catalysis, RSC Publishing, 2013, 1-58.):

$$H(T) = E_{elec} + E_{ZPE} + \int_{0K}^{T} C_v d\tilde{T} \quad \text{(Equation S1)}$$

$$E_{ZPE} = \frac{1}{2}\sum_{i=0}^{\#DOF} h\nu_i \quad \text{(Equation S2)}$$

$$\int_{0K}^{T} C_v d\tilde{T} = \sum_{i=0}^{\#DOF} \frac{h\nu_i}{e^{h\nu_i/k_BT}-1} \quad \text{(Equation S3)}$$

The results were presented in the Table S1. By comparing $\Delta E_{elec}$ and $\Delta H$, we concluded that temperature has little effect on the reaction energy (≤ 0.11 eV).

Table S3. Structure parameters as carbon coverage variation on (4×4) Fe(110)

| ML | | r(Fe-C)[a]/Å | r(Fe-C)[b]/Å | r($Fe_{sub}$-C)[c]/Å | ∠Fe-Fe-Fe | r(Fe-Fe)/Å |
|---|---|---|---|---|---|---|
| 0.00 ML/C | | | | | 70.53° | 2.452 |
| 0.0625 ML/C | C | 1.797, 1.797 | 1.955, 1956 | 2.392 | 84.51° | 2.578 |
| 0.25 ML/C | $C^1$ | 1.790, 1.790 | 1.954, 1.954 | 2.606 | 83.41° | 2.507, 2.507, 2.507,2.507 |
| | $C^2$ | 1.789, 1.790 | 1.954, 1.953 | 2.604 | 83.42° | 2.508, 2.508, 2.508,2.508 |
| | $C^3$ | 1.790,1.789 | 1.954, 1.954 | 2.603 | 83.40° | 2.508, 2.508, 2.507, 2.508 |
| | $C^4$ | 1.790, 1.790 | 1.954, 1.953 | 2.606 | 83.41° | 2.507, 2.507, 2.507, 2.507 |
| 0.25 ML/C +0.75 ML/H | $C^1$ | 1.764, 1.770 | 1.858, 1.904 | 2.013 | | 2.570, 2.566, 2.591, 2.595 |
| | $C^2$ | 1.733, 1.757 | 1.920, 1.941 | 2.535 | | 2.519, 2.499, 2.466, 2.538 |
| | $C^3$ | 1.738, 1.736 | 1.872, 1.928 | 2.066 | | 2.557, 2.512, 2.670, 2.552 |
| | $C^4$ | 1.877, 1.812 | 1.893, 1.911 | 1.853 | | 2.473, 2.630, 2.607, 2.487 |
| C/(2×2)(110)[1] | | 1.787 | 1.955 | 2.594 | | |

(a) Fe-C distance along the short diagonal line. (b) Fe-C distance along the long diagonal line. (c) Fe-C distance of C and subsurface Fe

Table S4 Comparison of the barriers and reaction energies under high and low coverage

| High coverage | | | Low coverage[2] | | |
|---|---|---|---|---|---|
| Reaction | $E_a$/eV | $E_r$/eV | Reaction | $E_a$/eV | $E_r$/eV |
| CH+CH+12H+2C→CHCH+12H+2C | 0.49 | −0.36 | CH+CH→CHCH | 0.61 | −0.36 |
| CH+CH+12H+2C→$CH_2$+CH+12H+2C | 0.52 | 0.44 | CH+H→$CH_2$ | 0.74 | 0.71 |
| $CH_2$CH+12H+2C→$CH_2CH_2$+11H+2C | 0.52 | −0.17 | $CH_2$CH+H→$CH_2CH_2$ | 0.72 | 0.36 |
| $CH_2CH_2$+12H+2C→$CH_2CH_3$+11H+2C | 0.51 | 0.15 | $CH_2CH_2$+H→$CH_2CH_3$ | 0.65 | 0.51 |
| $CHCH_3$+12H+2C→$CH_2CH_3$+11H+2C | 0.60 | 0.13 | $CHCH_3$→$CH_2CH_3$ | 0.80 | 0.39 |
| $CH_2CH_3$+12H+2C→$CH_3CH_3$+11H+2C | 0.72 | −0.58 | $CH_2CH_3$+H→$CH_3CH_3$ | 1.13 | 0.28 |

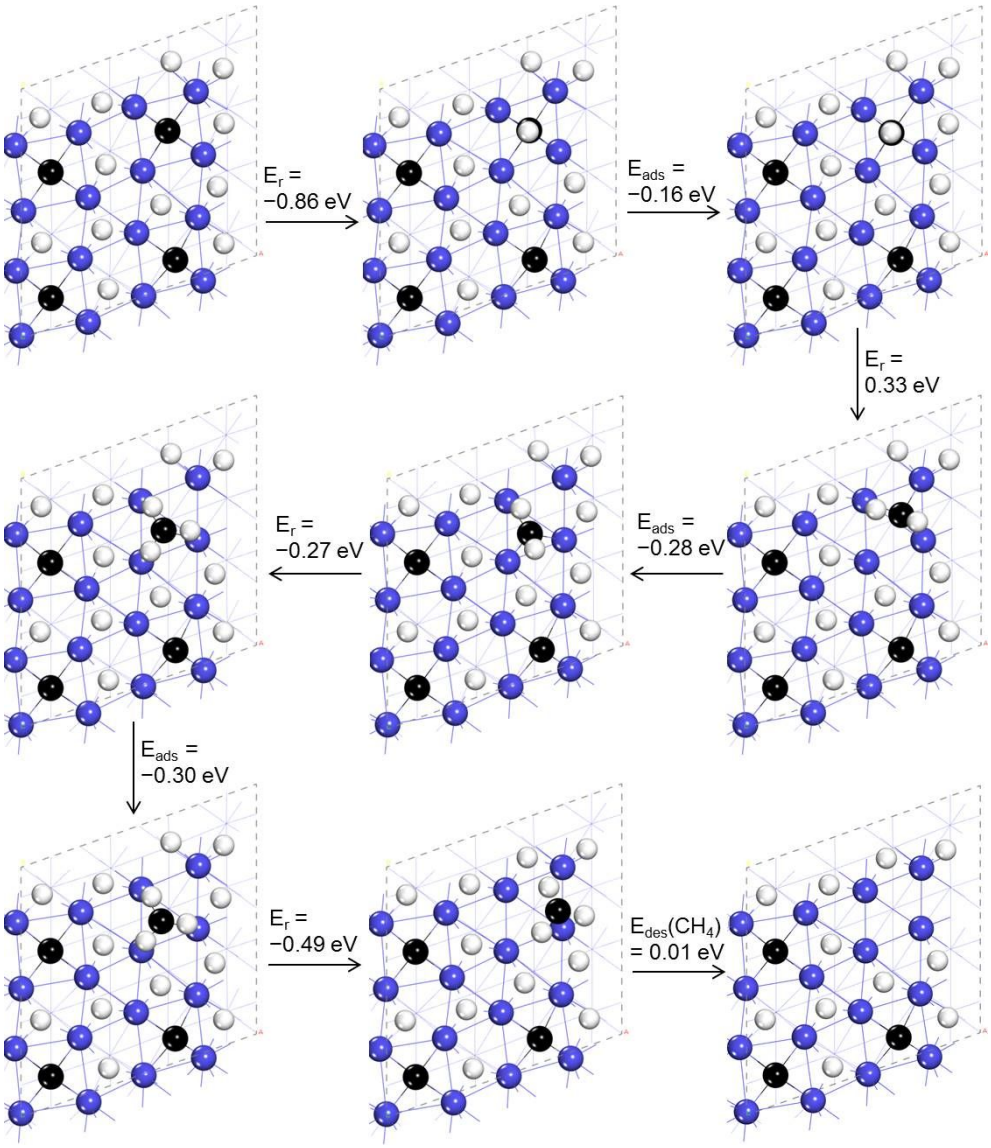


Figure S1 Thermodynamic properties of stepwise hydrogenation to methane of surface carbon including hydrogen adsorption and methane desorption

Note: blue balls are iron, black balls are carbon and white balls are hydrogen

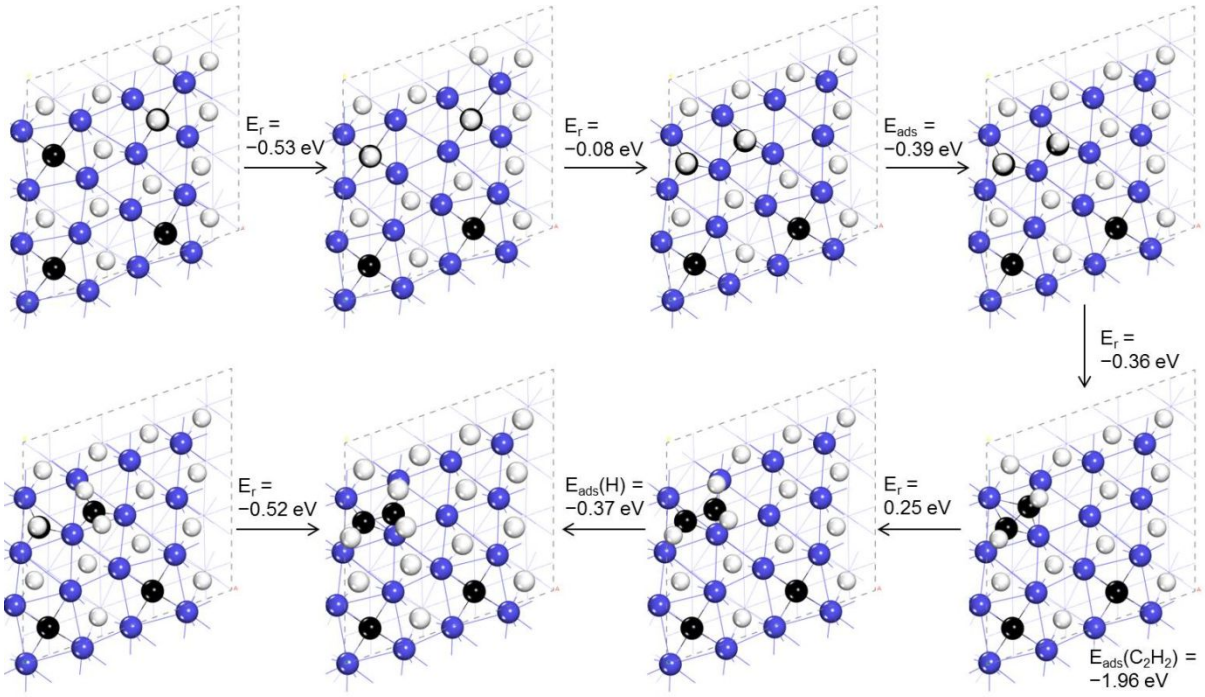


Figure S2 Thermodynamic properties of CH-CH coupling and hydrogenation to $CH_2CH$ as well as $CH_2$+CH coupling

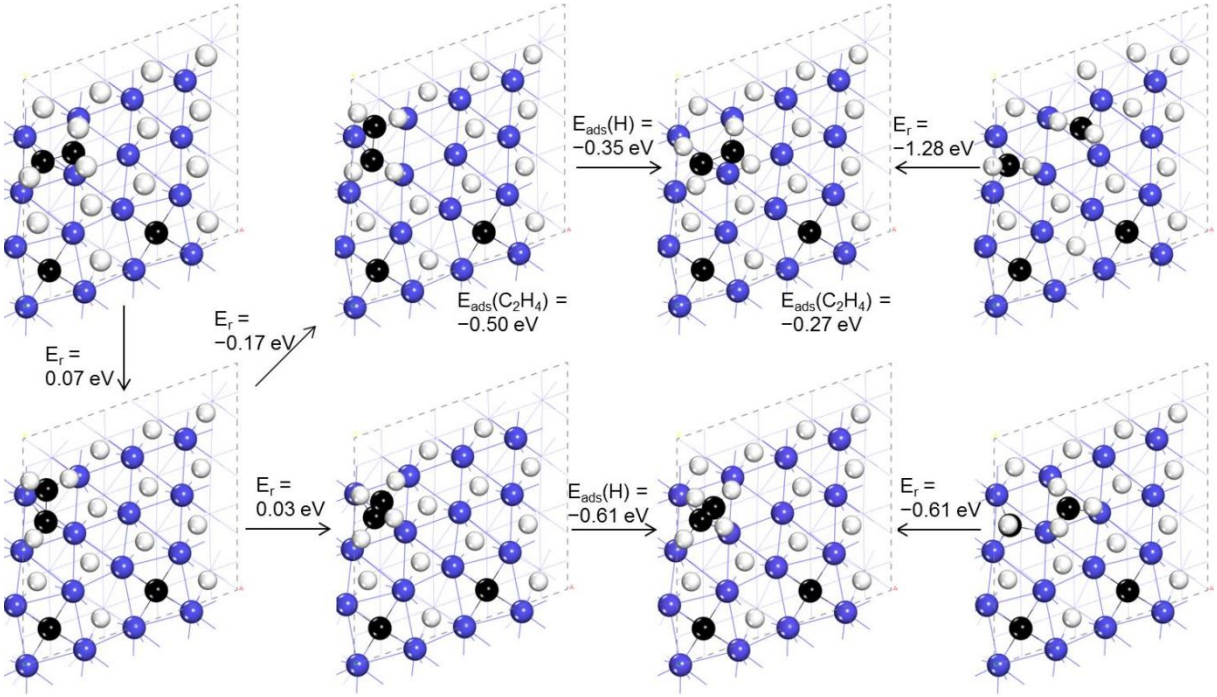


Figure S3 Thermodynamic properties of ethylene and $CH_3CH$ formation

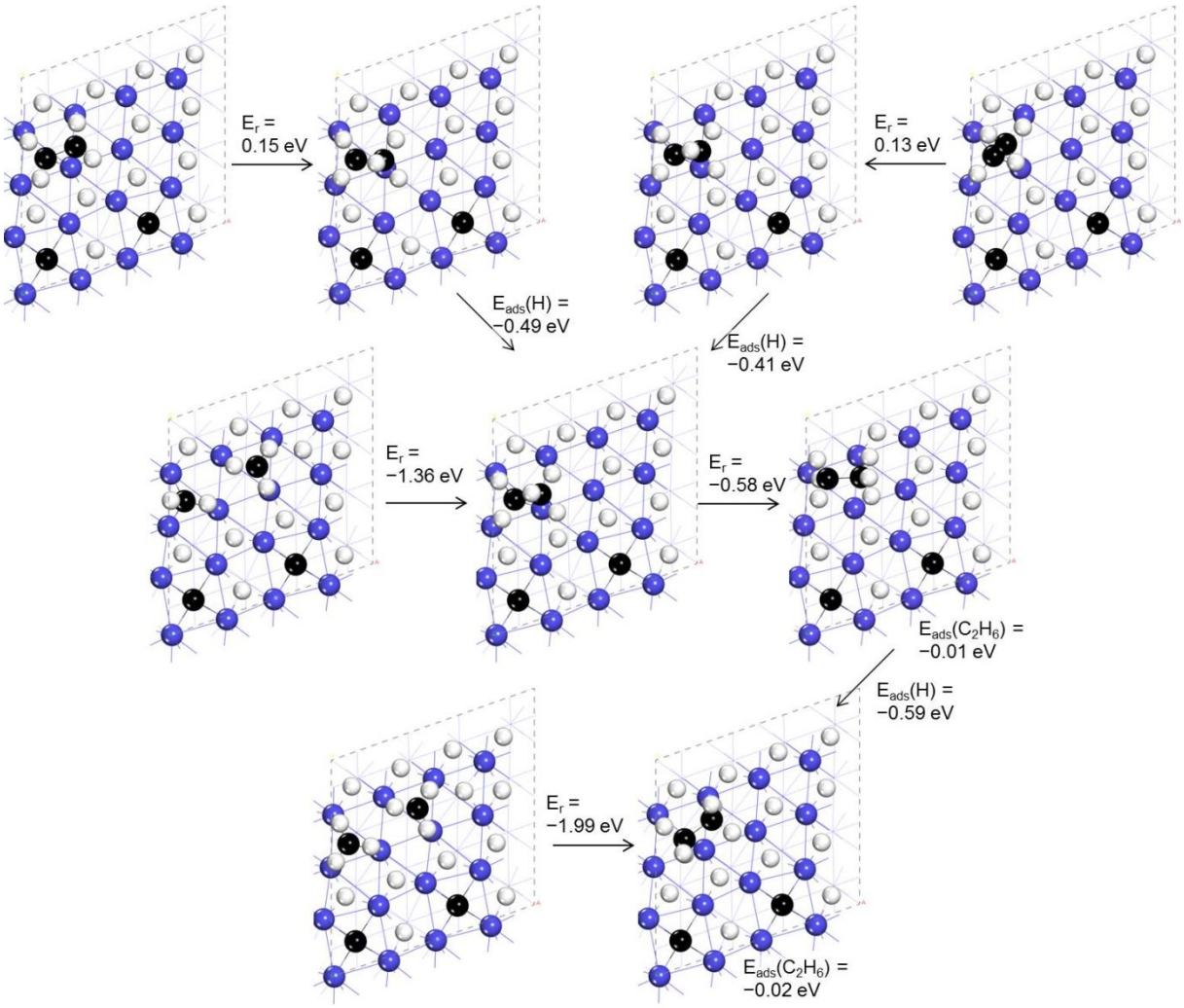


Figure S4 Thermodynamic properties of ethylene stepwise hydrogenation to ethane and coupling of two $CH_3$

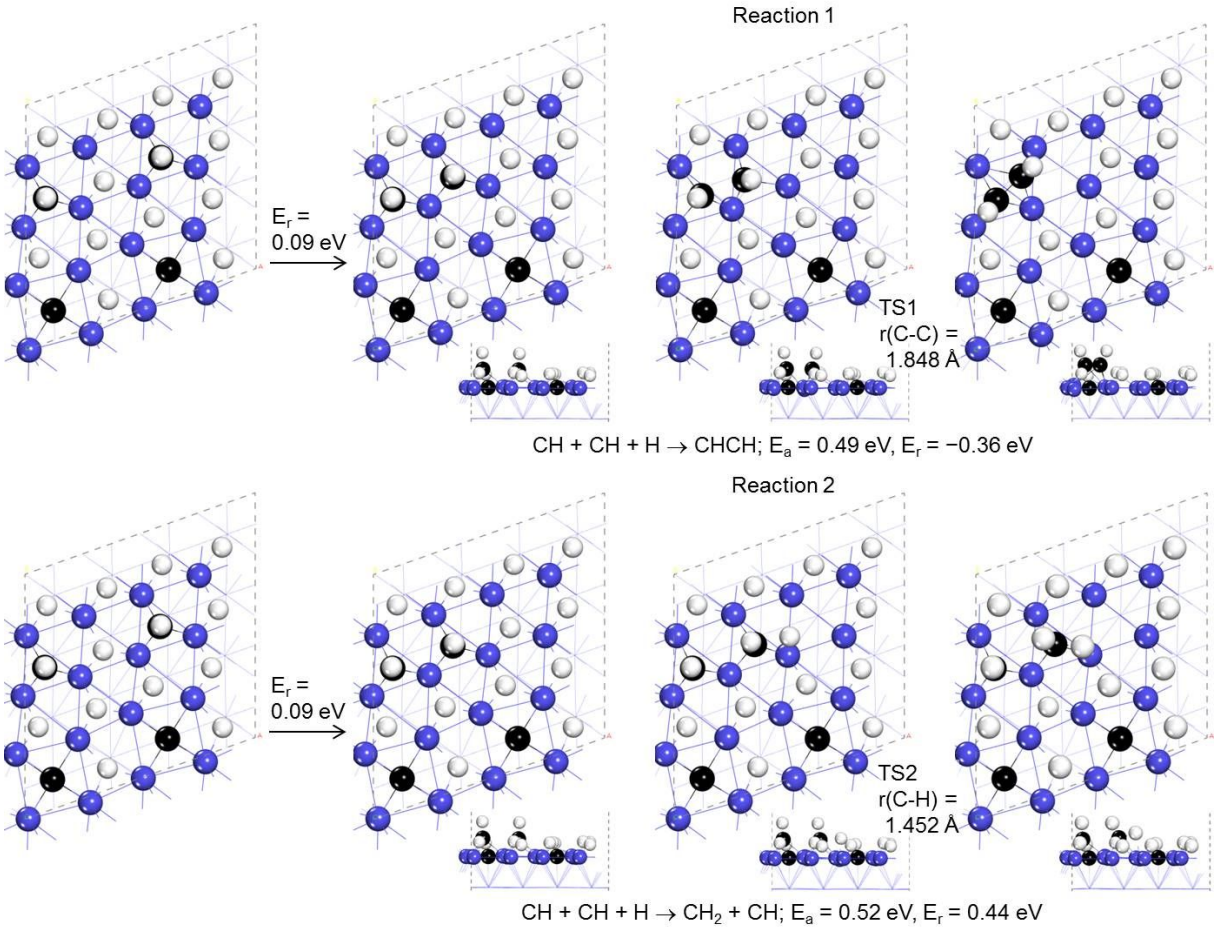


Figure S5 Reactions of CH+CH coupling to acetylene and CH hydrogenation

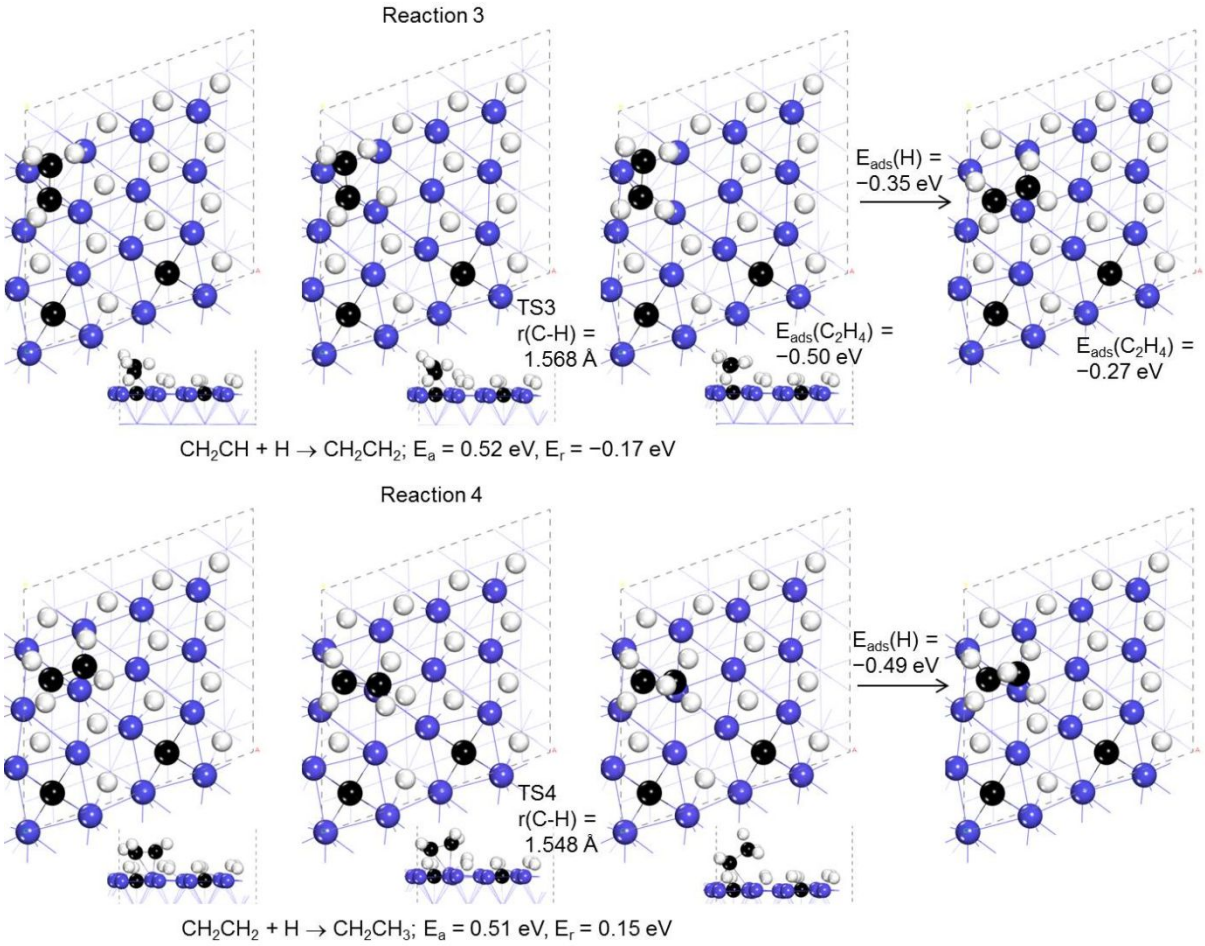


Figure S6 First hydrogenation path from $CH_2CH$ to $CH_2CH_2$ and $CH_2CH_3$

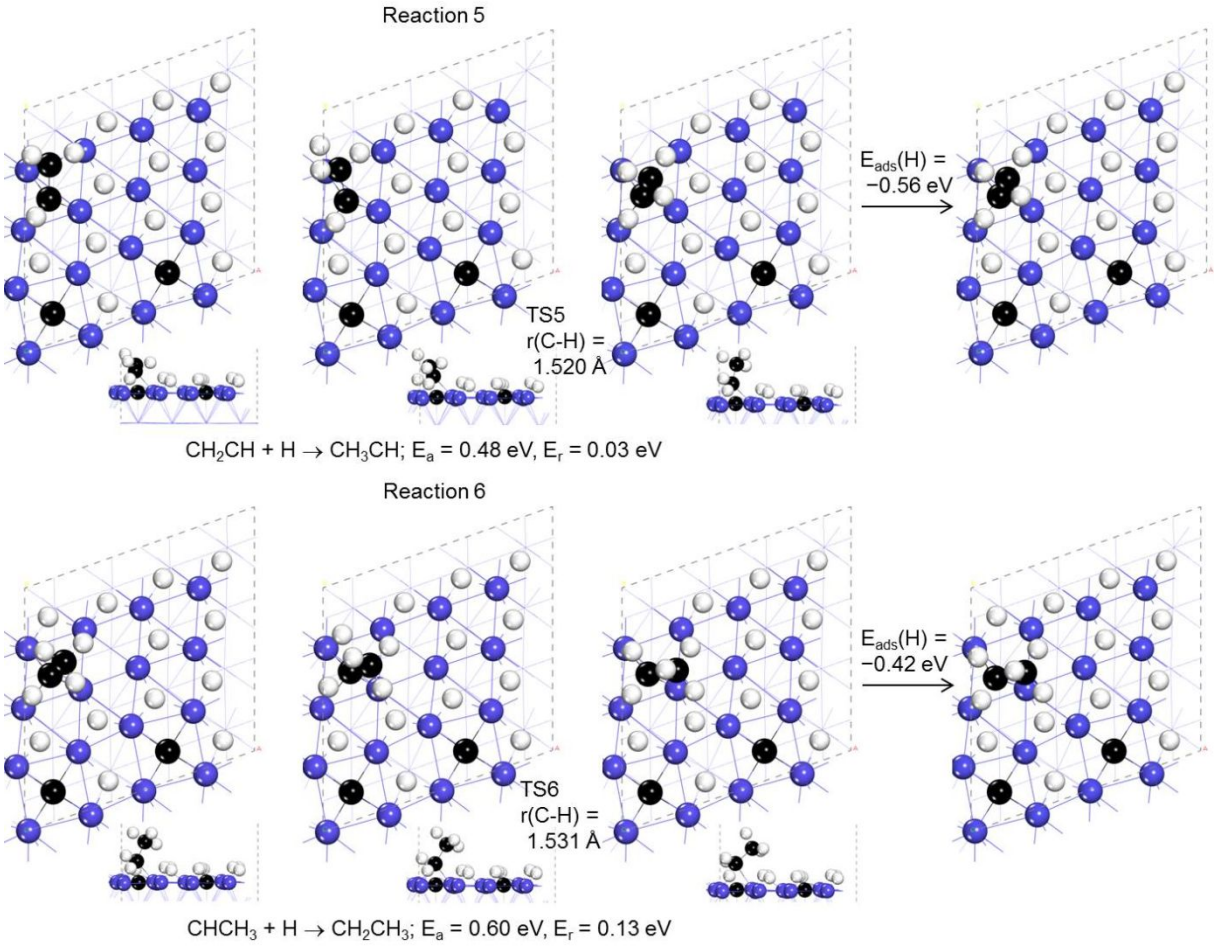


Figure S7 Second hydrogenation path of $CH_2CH$ to $CH_3CH$ and $CH_3CH_2$

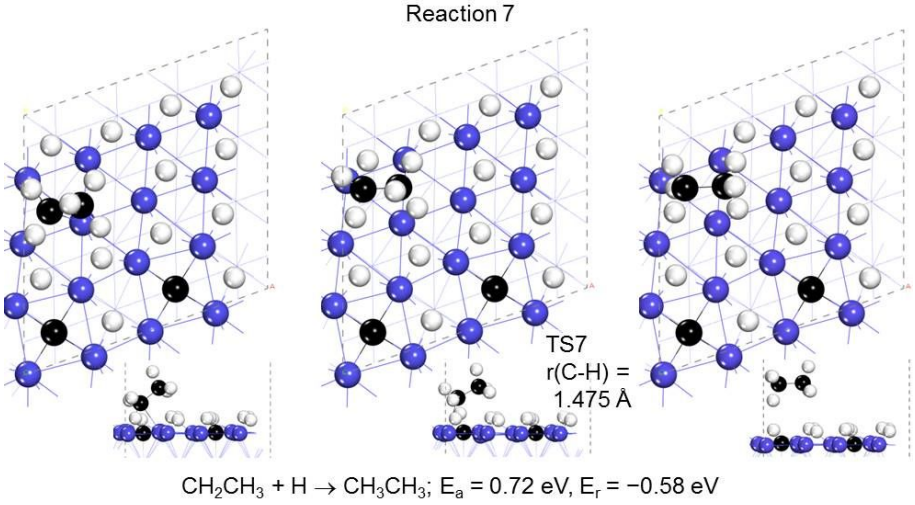


Figure S8 Ethane formation via ethyl hydrogenation

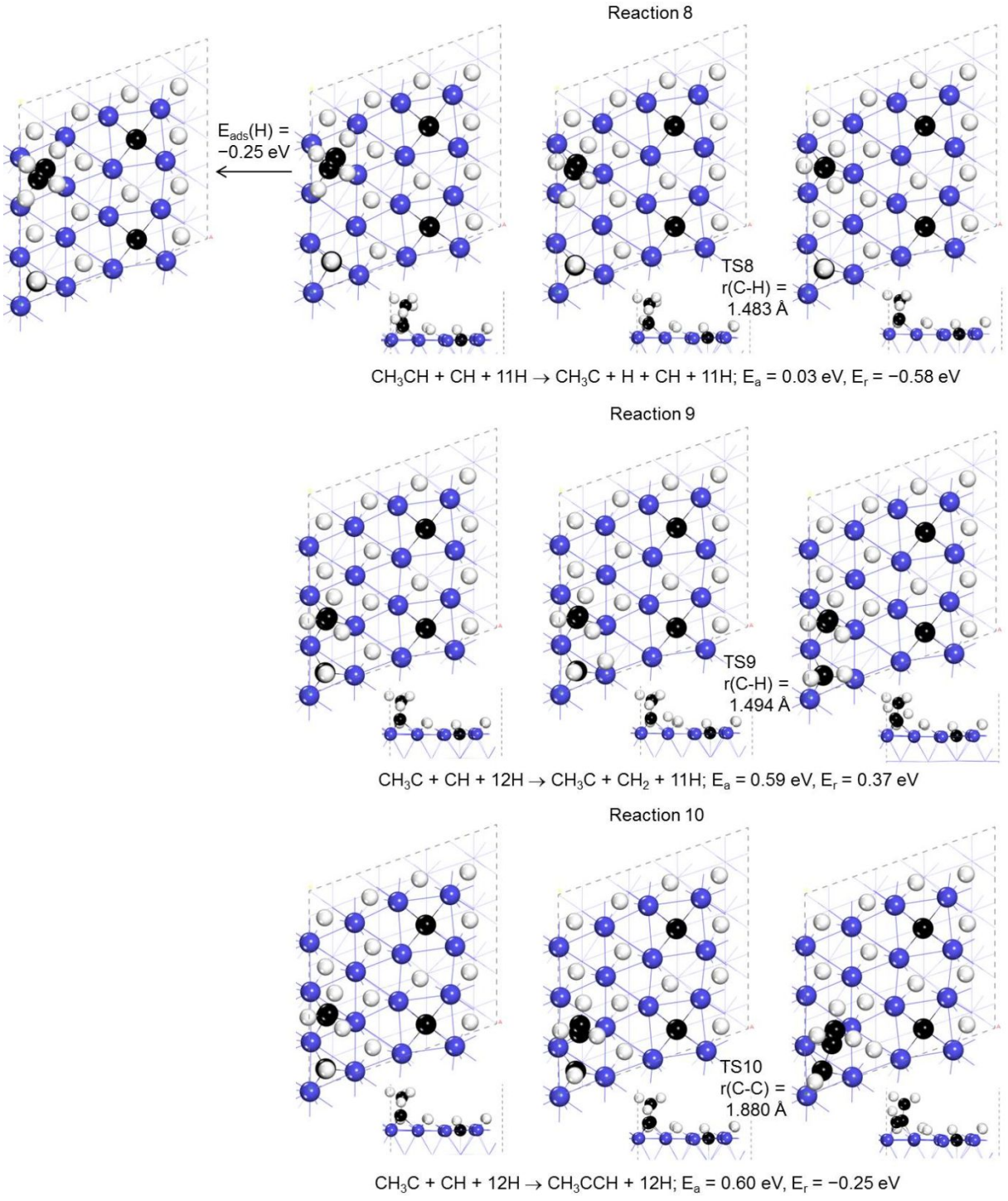


Figure S9 Dehydrogenation of $CH_3CH$ to $CH_3C$ and competition between CH hydrogenation and CH+$CH_3C$ coupling

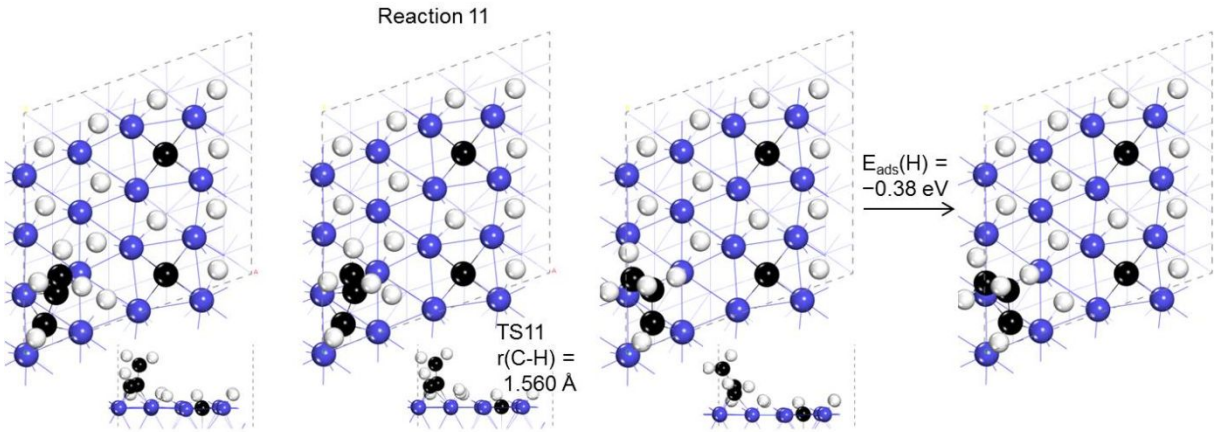


$CH_3CCH + 12H \rightarrow CH_3CHCH + 11H$; $E_a = 0.49$ eV, $E_r = 0.31$ eV

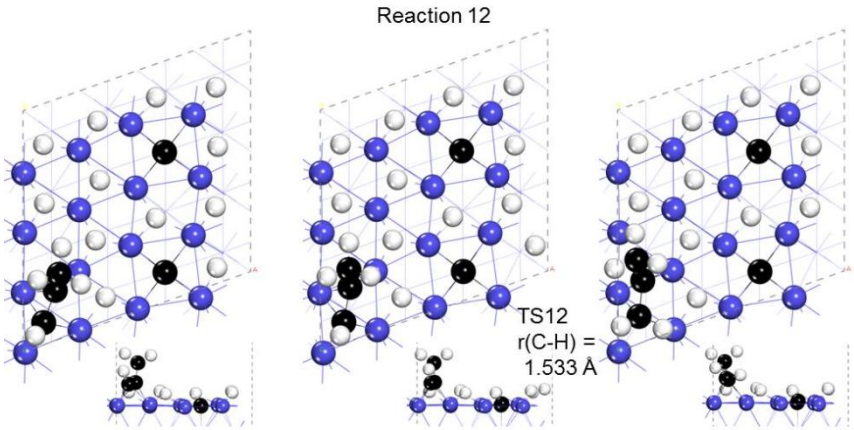


$CH_3CCH + 12H \rightarrow CH_3CCH_2 + 11H$; $E_a = 0.82$ eV, $E_r = 0.33$ eV

Figure S10 Competition of hydrogenation at middle and terminal carbon of $CH_3CCH$

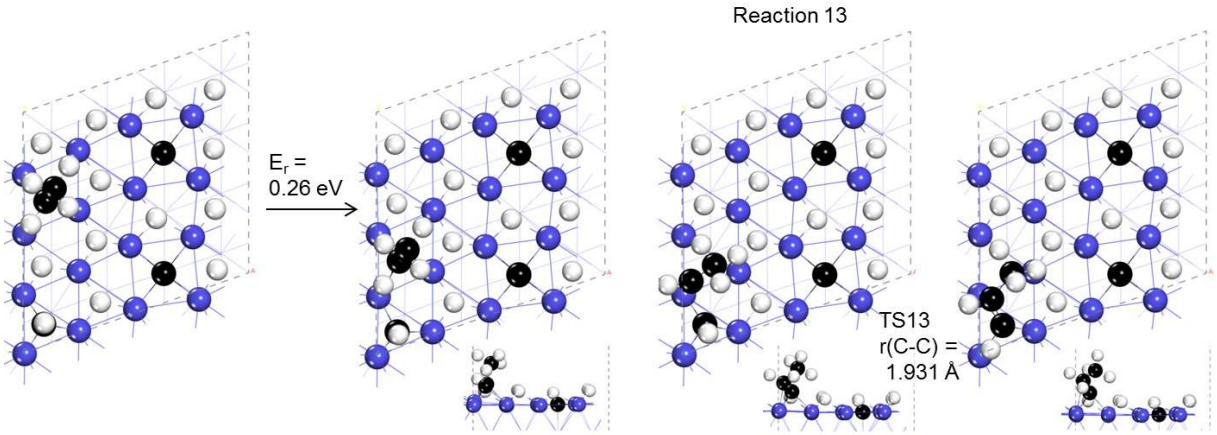


$CH_3CH + CH \rightarrow CH_3CHCH$; $E_a = 0.73$ eV, $E_r = -0.44$ eV

Figure S11 Formation of propenyl via direct C-C coupling

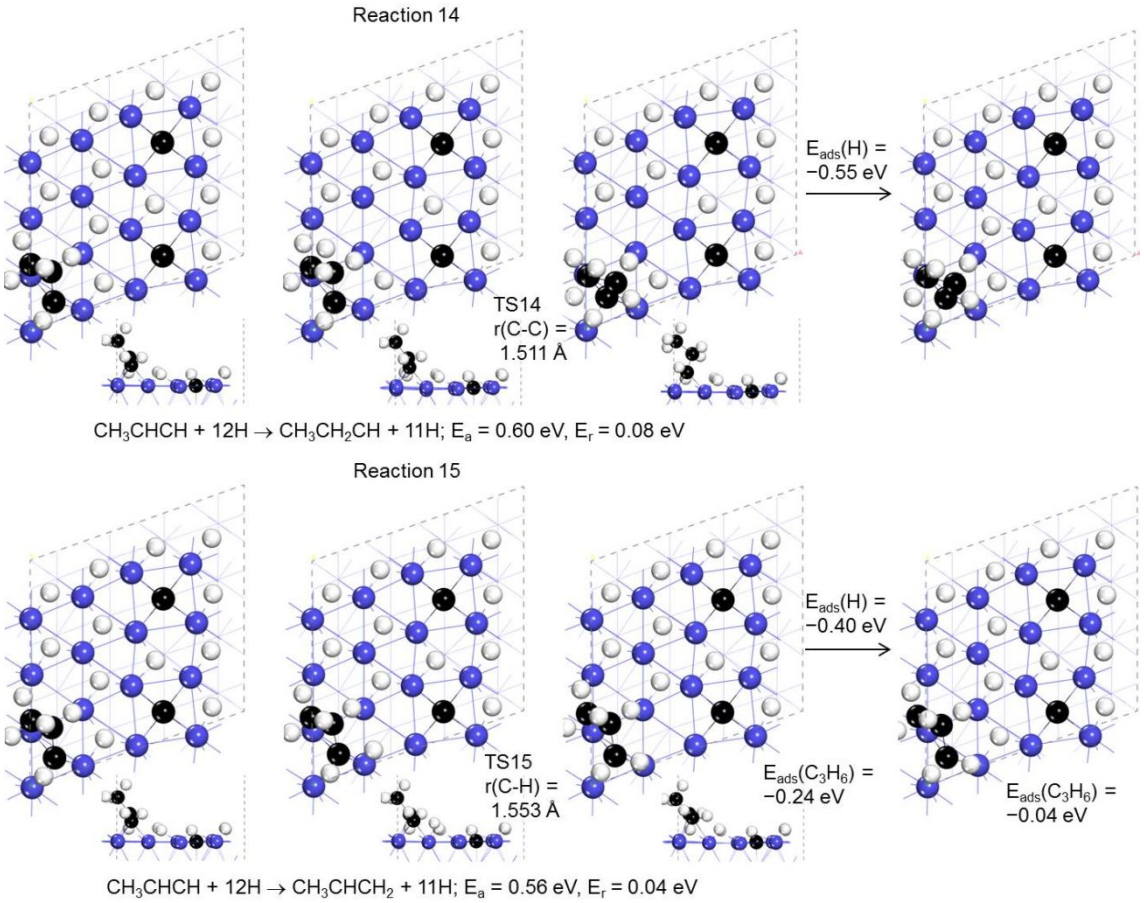


Figure S12 Competition of $CH_3CHCH_2$ and $CH_3CH_2CH$ formation of $CH_3CHCH$ hydrogenation

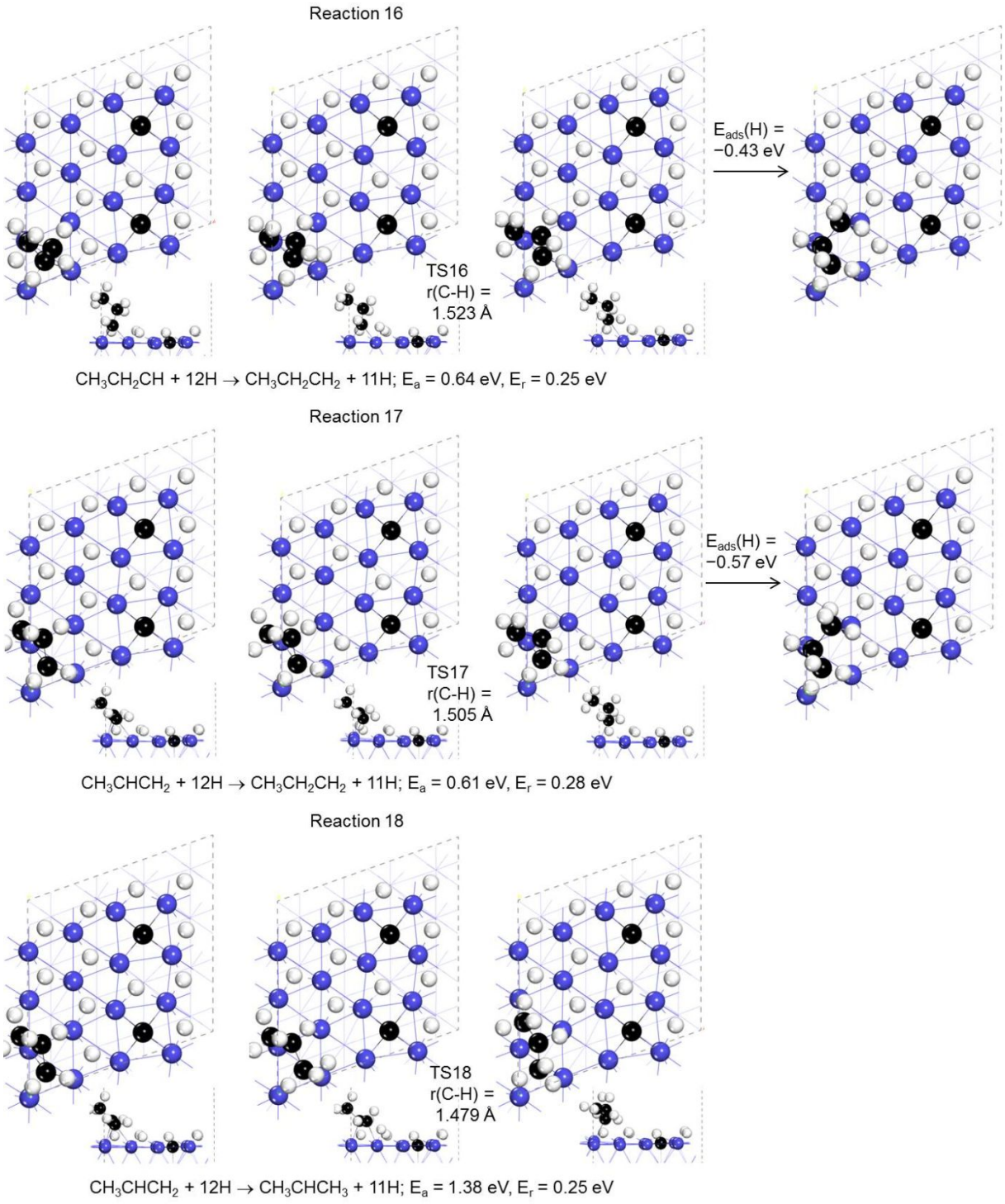


Figure S13 $CH_3CH_2CH$ hydrogenation to propyl and competitive hydrogenation of $CH_3CHCH_2$ to $CH_3CH_2CH_2$ and $CH_3CHCH_3$

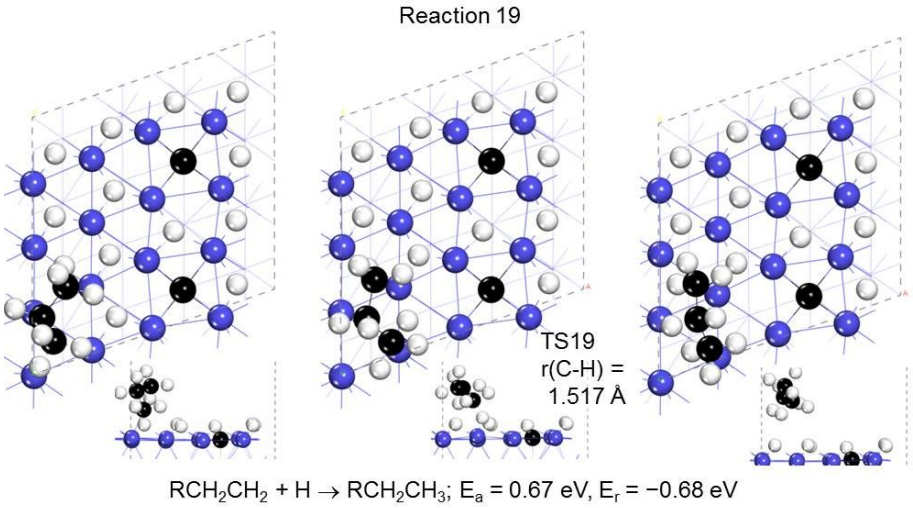


Figure S14 Propane formation via propyl hydrogenation

Reference

(1) Liu, X.-W.; Huo, C.-F.; Li, Y.-W.; Wang, J.; Jiao, H., Energetics of Carbon Deposition on Fe(100) and Fe(110) Surfaces and Subsurfaces. *Surf. Sci.* **2012,** 606, 733-739.

(2) Li, T.; Wen, X.; Li, Y.-W.; Jiao, H., Successive Dissociation of CO, $CH_4$, $C_2H_6$, and $CH_3CHO$ on Fe(110): Retrosynthetic Understanding of FTS Mechanism. *J. Phys. Chem. C* **2018,** 122, 28846-28855.